

Ballistic-Electron-Emission Microscopy and Spectroscopy of GaP(110)-Metal Interfaces

M. Prietsch^(a) and R. Ludeke

IBM T. J. Watson Research Center, Yorktown Heights, New York 10598

(Received 31 August 1990)

Ballistic-electron-emission-microscopy (BEEM) studies of Mg, Ni, Cu, Ag, and Au films on cleaved *n*-type GaP(110) show uniform Schottky-barrier heights across the surfaces, which varied from 1.02 eV for Mg to 1.41 eV for Au. BEEM images reveal areas of sharp current variations (contrast) that coincide with topographic gradients on the metal surfaces. Deduced Schottky-barrier heights depend on the transport model; a $\frac{1}{2}$ power-law dependence of the BEEM current on applied voltage results if nonclassical transmission across the interface is included.

PACS numbers: 73.40.Gk, 61.16.Di, 68.55.Jk, 73.30.+y

Ballistic-electron-emission microscopy (BEEM) is a recently developed scanning-tunneling-microscope-based technique that allows the determination of changes in the potential at semiconductor interfaces with previously unattainable lateral resolution.^{1,2} Such changes may arise from potential steps at a metal-semiconductor (MS) interface (Schottky barrier), and are manifested by an onset of current in the semiconductor as the tunneling tip bias exceeds the Schottky-barrier height.¹ Previous investigations, which generally lacked ultrahigh vacuum (UHV) and *in situ* preparation facilities, were limited in the choice of metal and substrate preparation.¹⁻⁴ We report here BEEM studies of Mg, Ni, Cu, Ag, and Au overlayers on cleaved *n*-type GaP(110) surfaces. Cleaves, metal depositions, and measurements were made consecutively in UHV without intervening air exposures. Our principal conclusions are (1) Schottky-barrier heights vary from 1.02 eV for Mg to 1.41 eV for Au; (2) for a given metal, barrier heights at diverse locations were constant to within ± 0.02 eV; (3) observed variations in collector or BEEM current (I_c) are attributed to topographic gradients on the metal surface, and *not* to variations in Schottky-barrier heights, as stipulated for GaAs and Si.^{1,2} Thus contrast in BEEM images is strongly dependent on the surface topography. In addition, we have modeled the electron transport across the interface by including an energy-dependent transmission coefficient.

The scanning tunneling microscope, specifically designed for BEEM studies in an UHV environment,⁵ consists of a tubular piezoelectric scanner mounted horizontally on a sled that is pushed by a Burleigh Inchworm for coarse approach. The removable tunneling tip can be cleaned by electron bombardment on an adjacent stage, which also houses three additional spare tips. Two other Inchworms position the bias electrode on the metal for BEEM experiments. Vibration isolation is achieved by a dual-stage spring suspension plus eddy-current damping. A removable sample holder allows for varied sample preparations in an adjacent, vacuum interlocked preparation and analysis chamber. In the present case, *n*-type

GaP(110) (Te doped to 2×10^{17} cm⁻³) surfaces were prepared by cleavage in UHV, followed by immediate metal deposition through a mask. We used 2-mm-diam metal dots, whose thickness varied from 30 to 200 Å.

A preferred mode of computer-controlled data acquisition consisted of topographic scans interrupted at a predetermined array of points evenly distributed over the scanned area; at each grid point I_c was taken as a function of the tip-to-metal bias voltage, with the tip current held typically at 1 nA. Many such I - V arrays were taken for each sample; a minimum of two samples were fabricated for each metal-GaP combination. Representative BEEM I - V curves for Mg, Ni, Cu, Ag, and Au on *n*-type GaP(110) are shown, vertically shifted for display purposes, in Fig. 1, together with fits (solid curves) that will be discussed later. Each of these curves, which were smoothed by averaging over several adjacent points, represents a single scan out of an array of typically sixteen I - V curves. A definite range in the onset of I_c is clearly apparent. The I - V curves were taken under feedback control with a tip current of 1 nA, with the exception of Ni, for which 5 nA was used. I_c for Ni was reduced to $\frac{1}{5}$ in Fig. 1. The relative BEEM current intensities reflect the role of the electron transmission through the metals, although variations in the transmission coefficients across the interfaces may contribute as well. From the numerous sets of I - V curves taken for the five metals we have made the following observations: (1) an essentially common value for the threshold voltage for a given metal-GaP contact, (2) occasional sudden jumps in I_c , and (3) pronounced differences by factors of up to 5 in I_c at different positions of the sample surface. The latter two phenomena are illustrated in Fig. 2 for Au on GaP. Curve *a* depicts sudden changes in the BEEM current, which in this particular case first drops and then returns to its original "trajectory." Curves *b* and *c* represent two I - V curves taken in the same scan sequence under identical conditions, but at different locations on the surface that differ only by their relative inclination to the average surface plane, here 0° and 10°, as determined from a topographical cross section at the point of

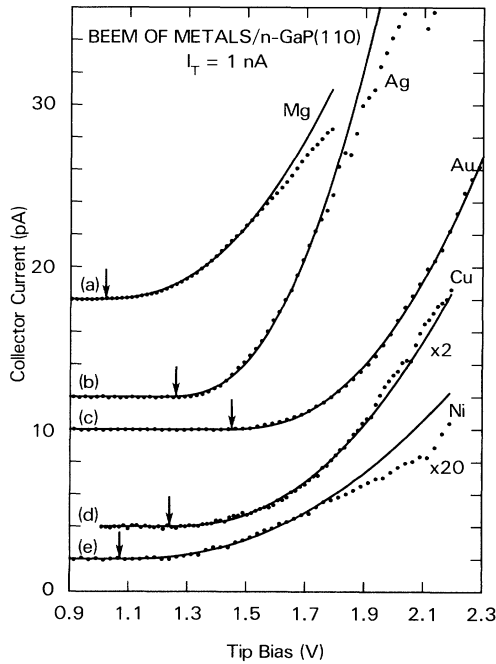


FIG. 1. BEEM I - V spectra (dots) for curves *a*, 80 Å Mg; *b*, 200 Å Ag; *c*, 60 Å Au; *d*, 150 Å Cu; *e*, 50 Å Ni. Arrows mark current threshold obtained from fits (solid curves) with Eq. (1).

data acquisition. We will demonstrate here that both phenomena are related to surface topography, specifically variations in surface gradients, and *not* to variations in film thickness. The latter were typically 10%–15% of total film thickness, which is insufficient to explain the large variations in I_c . To emphasize this point, one need only compare I_c at a given bias for two metal thicknesses, as shown in Fig. 2 for Au overlayers of 120 Å (dots, curve *b*) and 60 Å (triangles). Both curves represent spectra of high current intensity measured on flat areas of the two samples. Thus a 50% reduction in the thickness of the Au layer merely increases I_c by $\approx 12\%$ for a tip bias of 2 V, a change that indicates an electron mean free path (~ 500 Å) that is much larger than the thickness fluctuations. Thus current loss due to inelastic scattering in the metal film does not account for the observed differences among spectra on the same sample, such as those in curves *b* and *c* of Fig. 2.

Our alternative explanation is based on the observed surface roughness, which may cause the electron injection to be off normal to the average film plane. This occurs when the tunneling tip scans over an inclined surface area, for which the injected electrons will have a predominant wave vector in the direction of the local surface normal. Hence the injected electrons, assumed to ballistically traverse the metal film, will be inclined at a similar angle when they reach the interface. Unless elastically scattered, these electrons have a reduced “for-

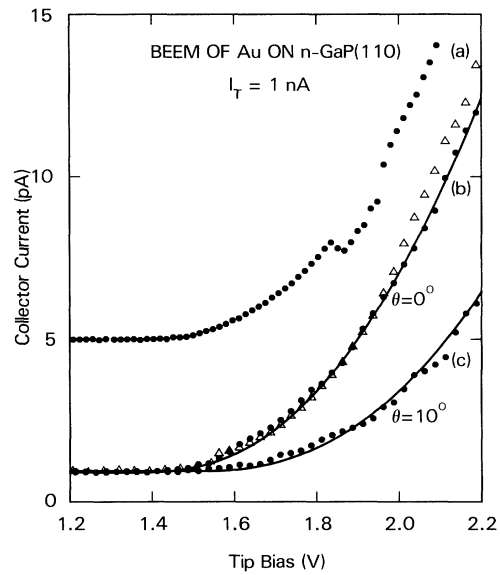


FIG. 2. Frequently observed current variations in BEEM I - V spectra (dots) and their fits (lines) for a 120-Å Au film. The triangles represent data for a 60-Å Au film.

ward” energy of momentum component normal to the interface. This reduction may be sufficient to prevent the electron from crossing the barrier (total reflection), or in the very least diminish its transmission probability. The sudden jumps in BEEM current, as illustrated in Fig. 2, curve *a*, are attributed to small drifts of the tip over topographically rough areas, possibly accompanied by changes of the local tunneling asperity of the tip. The resulting structure in the I - V spectra can at times be quite subtle and appear to be reproducible as well. However, from the extensive number of spectra measured we found that all semblances of structure in the I - V curves were attributable to such tip effects. The frequency of current fluctuations correlated with the surface roughness, being largest for Ni, with a decreasing tendency observed for Cu, Au, Ag, and Mg. The latter exhibited the smoothest surface topography of the five metals, as shown in Fig. 3(a), and by far the most reproducible and structure-free I - V spectra.

A dramatic illustration of the role of surface topography on I_c , and hence BEEM image contrast, is shown in Fig. 3 for a 200-Å Mg layer on *n*-type GaP(110). This triptych consists of (a) the topographic image of the Mg surface, (b) the absolute value of the first derivative of this image, which delineates areas of steepest slope—shown here in white—that appear to be associated with grain boundaries, and (c) the BEEM image, with the darker shading corresponding to low I_c . An exact spatial correspondence exists between the pattern of high topographic surface gradients in (b) and that for low collector current in the BEEM image. Some small areas of low current, such as the spots left of center in (c), which

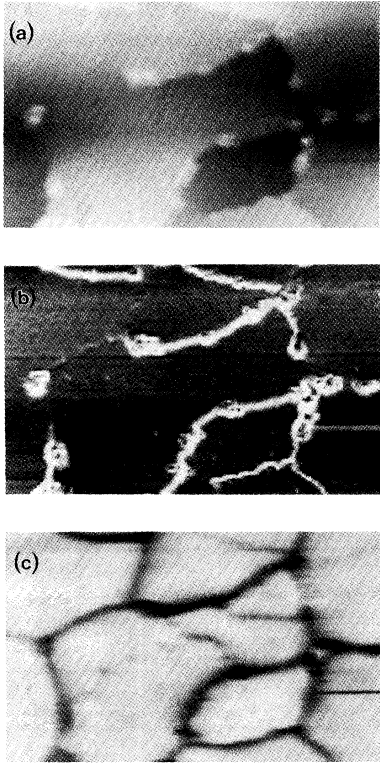


FIG. 3. 200-Å Mg film on GaP(110): (a) topographic image of $600 \times 400 \text{ \AA}^2$ area, (b) gradient image of (a), and (c) simultaneously collected BEEM image. $V = 2.0 \text{ V}$, $I_T = 5 \text{ nA}$. Black-white contrast scale: (a) 12 Å, (b) 0%–30%, (c) 8–28 pA.

do not match obvious topographic features in (a) or (b), may arise from morphological or compositional inhomogeneities of unknown origin at the interface. Nevertheless, we conclude that the principal contrast in BEEM images arises from topographic surface features of the metal overlayer. We observe similar results for the other metals; however, their larger surface roughness causes instabilities in I_c which adversely affects the quality of the BEEM images.

In order to obtain an accurate value of the threshold voltage V_0 , and hence the Schottky-barrier height, some basic assumptions on the nature of the tunneling and transport processes must be made to derive a useful functional dependence of the collector current on the applied voltage V near threshold V_c . Bell and Kaiser² have proposed a model, based on planar tunneling theory,^{6,7} for the transmission across an MS interface that assumes an energy-independent (classical) transmission probability. Their model predicts $I_c \propto (V - V_0)^2$ near threshold. The model is within the framework of the effective-mass approximation and assumes, besides transverse momentum conservation, that both the metal and semiconductor conduction-band extrema lie at the Brillouin zone (BZ) center. The latter condition is satisfied for hole transport in all, and for electron transport in most tetrahedrally coordinated semiconductors, notable exceptions being Si, Ge, AlAs, and GaP. However, for interfaces of orientations corresponding to directions to the conduction-band minima in k space, e.g., both (100) and (110) surfaces of Si and GaP, the condition for a zone-centered band is still met because conservation of crystal momentum is relaxed in that direction: Along the [110] reciprocal-lattice direction, an X -point conduction-band minimum exists in the second BZ that maps onto the $\bar{\Gamma}$ zone center of the (110) surface BZ. Consequently, from a point of view of transport across the interface, GaP(110) can be treated as a “direct” band-gap material, which exhibits, however, an anisotropic mass.

In contrast to the assumption by Bell and Kaiser² of a classical transmission factor at the MS interface, we want to explore here the consequences of an energy-dependent transmission coefficient $T(E)$ on data fits and threshold values. We will use a generalization of the quantum-mechanical transmission coefficient across a one-dimensional potential step with boundary conditions that conserve current.⁸ For $m_s \ll m$, where m_s and m are the effective-mass components of the semiconductor and metal in the direction normal to the interface, or for $E_F \gg e(V - V_0)$, where E_F is the Fermi energy of the metal relative to the bottom of the conduction band, the transmission factor becomes

$$T(E_x, E_t) \approx 4 \{ [mm_s(E_x - E_F + eV - eV_0) - m(m - m_s)E_t] / m_s^2(eV + E_x) \}^{1/2}.$$

E_x and E_t are energy variables with respective momentum components perpendicular and parallel to the interface.^{2,7} For simplicity, we assume an isotropic effective mass for the semiconductor [$m_s = (m_l^2 m_t)^{1/3} = 0.36m$ for the X point of GaP (Ref. 9)], as well as the same Fermi energy and (free) electron mass for the tunneling tip and the metal overlayer. Inclusion of $T(E)$ in the collector current integral [see Eq. (4) of Ref. 2] yields the following expression for the collector current density j_c :

$$j_c \approx Ke^{-A\phi^{1/2}} \left\{ \frac{(eV - eV_0)^{5/2}}{(E_F + eV_0)^{1/2}} \left[1 - \frac{2}{7} \rho e(V - V_0) + O((eV - eV_0)^2) \right] \right\}, \quad (1)$$

where $A = 2d(2m)^{1/2}/\hbar$, $\rho = A/2\phi^{1/2}$, and $\phi = \bar{\phi} - V/2$. $\bar{\phi}$ represents the average height of a rectangular tunnel barrier of width d .^{6,7} K is a scaling factor that includes attenuation due to electron scattering in the metal film. Thus Eq. (1) predicts a $(V - V_0)^{5/2}$ dependence near threshold that differs from the previously proposed² square law by the $\frac{1}{2}$ order derived from the transmission coefficient $T(E)$. Since the model does not consider details of the band structure and

TABLE I. Schottky-barrier values, in eV, for *n*-type GaP(110) deduced from fits of BEEM *I-V* curves.

Fit	Mg	Ni	Cu	Ag	Au
Eq. (1)	1.03	1.06	1.21	1.26	1.41
"Square"	1.08	1.14	1.27	1.30	1.45
Error	± 0.02	± 0.03	± 0.02	± 0.02	± 0.02

scattering processes, both of which affect mainly the magnitude and to a lesser extent the energy dependence of the transmission probability, the prefactor *K* represents a scaling parameter adjusted to fit the data.

For the fits to the experimental data the following steps were taken: (1) Temperature broadening was reinstated by convoluting the Fermi function numerically with dj_c/dV ; (2) E_F was calculated from published k_F values;¹⁰ (3) $\bar{\phi}$ was assumed to be the mean of the work functions of the tip (*W*) and the metal overlayer, and its width $d=10$ Å; and (4) to account for the constant-tunnel-current mode of data acquisition, which results in a slight increase in d with increasing bias voltage, Eq. (1) was normalized by dividing by $\phi - (\phi + eV) \times \exp(-eVA/2\phi^{1/2})$ (see Ref. 7). The fits were relatively insensitive to the choice of E_F , $\bar{\phi}$, and d . The solid curves in Fig. 1 and curve *b* in Fig. 2 are fits using Eq. (1); curve *c* in Fig. 2 was fitted with a modified Eq. (1) that includes the effects of off-normal angles of incidence of electrons reaching the interface.¹¹ The voltage thresholds or Schottky-barrier heights obtained from the fits are indicated by arrows. Their values are listed in Table I. For comparison, those obtained by assuming $j_c \propto (V - V_0)^2$ near threshold are also included. The thresholds fitted with Eq. (1) are systematically lower by 40–80 meV from those with "square-law" fits. The fits with the two different power laws were of comparable quality for $V - V_0 \lesssim 0.6$ eV, and thus cannot be used to distinguish between the two approaches. However, we would argue that a complete description of hot-electron transport across the interface should include nonclassical effects, as these are relevant in the related Si-NiSi₂.¹² Beyond these voltages both types of fits increasingly deviate from the experimental curves due to inelastic electron scattering in the metal, which points to the necessity of including an energy-dependent scattering formalism to improve the fits and perhaps discriminate between the two models. It should be emphasized here that all our fits were done with a single threshold. We could not fit the data with additional thresholds² due to higher-lying conduction-band minima, e.g., *L* at 0.18 eV above *X* and Γ at 0.51 eV above *X*.

The $\frac{5}{2}$ power law of Eq. (1) does not depend on the assumption of conservation of transverse momentum. A nearly identical expression, except for the prefactor, is obtained when momentum conservation is relaxed. For this case, transverse momentum is nevertheless restricted by the propagating states of the semiconductor conduction band, which, for small effective masses, means that only electrons with momentum normal or near normal to the interface will be collected. The presence of quasi-elastic scattering in the metal does not alter the criteria for transport in the semiconductor, and thus does not lead to a different power law near threshold. On the other hand, a dominance of this type of scattering either in the metal (phonons) or at the interface (roughness) implies that all sensitivity to surface topography (gradients) is lost, which is not observed experimentally. We may conclude from this that quasielastic scattering, either in the metal film or at the MS interface, is negligible for the metals on GaP(110) studied here. The question as to the degree of conservation of transverse momentum remains open.

We gratefully acknowledge the technical assistance of C. Candotti, R. Kaufman, F. Maurer, and M. Prikas, as well as valuable discussions with R. Feenstra, M. Lutz, C. K. Shih, A. Samsavar, M. Stiles, and J. Tersoff.

^(a)Permanent address: Institut für Experimentalphysik, Freie Universität Berlin, 1000 Berlin 33, Germany.

¹W. J. Kaiser and L. D. Bell, Phys. Rev. Lett. **60**, 1406 (1988).

²L. D. Bell and W. J. Kaiser, Phys. Rev. Lett. **61**, 2368 (1988).

³L. D. Bell, M. H. Hecht, W. J. Kaiser, and L. C. Davies, Phys. Rev. Lett. **64**, 2679 (1990).

⁴A. E. Fowell, R. H. Williams, B. E. Richardson, and T. H. Shen, Semicond. Sci. Technol. **5**, 348 (1990).

⁵M. Prietsch, A. Samsavar, and R. Ludeke, Phys. Rev. B (to be published).

⁶J. G. Simmons, J. Appl. Phys. **35**, 2655 (1964).

⁷E. L. Wolf, *Principles of Electron Tunneling Spectroscopy* (Oxford, New York, 1985), Chap. 2.

⁸D. J. BenDaniel and C. B. Duke, Phys. Rev. **152**, 683 (1966).

⁹J. C. Phillips, *Bonds and Bands in Semiconductors* (Academic, New York, 1973), p. 121.

¹⁰W. A. Harrison, *Electronic Structure* (Freeman, San Francisco, 1980).

¹¹R. Ludeke and M. Prietsch, J. Vac. Sci. Technol. (to be published).

¹²M. D. Stiles and D. R. Hamann, Phys. Rev. B **40**, 1349 (1989).

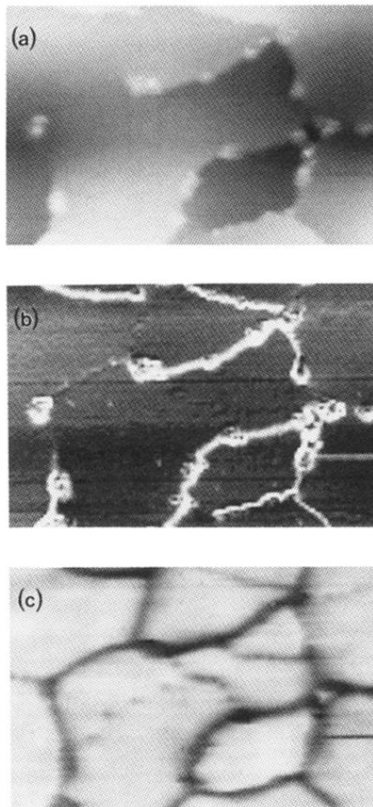


FIG. 3. 200-Å Mg film on GaP(110): (a) topographic image of $600 \times 400 \text{ \AA}^2$ area, (b) gradient image of (a), and (c) simultaneously collected BEEM image. $V = 2.0 \text{ V}$, $I_T = 5 \text{ nA}$. Black-white contrast scale: (a) 12 \AA , (b) 0%-30%, (c) 8-28 pA.